Electrosynthesis

Green Electrosynthesis of Hydroxylamines via CuS Suppressing N−O Bond Cleavage

Suisheng Li[+], Peisen Liao[+], Jiacheng Li[+], Pingping Jiang[+], Runan Xiang, and Guangqin Li*

Abstract: Organic hydroxylamines, pivotal intermediates in pharmaceutical and polymer chemistry, face persistent challenges in selective synthesis. Its main difficulty lies in the strong repulsion between the lone pair electrons on the N and O atoms, which makes their N−O bond easy to break, leading to a over-reduction to amine compounds. Here, we present a green electrocatalytic strategy for the first time that converts oximes to hydroxylamines over CuS. Specially, *N*-benzylhydroxylamine was achieved with 95% conversion and 80% selectivity from benzaldoxime at −0.9 V versus reversible hydrogen electrode. Mechanistic investigations reveal that CuS can optimize the adsorption energy of the reaction intermediates, making the N−O bond more difficult to cleave during the electrocatalytic hydrogenation, thus leading to a high selectivity formation of hydroxylamines. This methodology is successfully extended to other hydroxylamines and further enables the unprecedented synthesis of organic hydroxylamines from nitric oxide gas. Our work establishes a sustainable electrosynthetic platform for hydroxylamines synthesis without organic solvents and additional reduction agents, providing new insights for modern green chemical synthesis.

Introduction

Organic hydroxylamines, characterized by the N−O bond and versatile redox activity, serve as pivotal intermediates in pharmaceutical synthesis, agrochemical manufacturing, and functional polymer design.[1,2] Their unique structure enables applications as nitric oxide donors, antibacterial agents, and radical scavengers.[3,4] Despite their utility, the selective synthesis of primary hydroxylamines remains a formidable challenge due to inherent instability and competing pathways during traditional reductive processes.

One of the most conventional approaches to hydroxylamines production is catalytic hydrogenation of oximes by reducing reagent.[5] However, the route suffers from critical selectivity issues and low reactivity (Scheme 1). The hydrogenation of oximes typically proceeds through intermediates such as imines or transient hydroxylamines, ultimately yielding primary amines.[6] Precise control over the intermediate hydroxylamine stage remains elusive due to the strong repulsion between the lone pair electrons on the N and O atoms.[7] Notably, previous studies have identified several available methods that facilitate the efficient synthesis of hydroxylamines. Zhang et. al achieved high selective hydrogenation of oximes to hydroxylamines with nickel catalyst under H_2 reducing atmosphere based on weak interaction mechanism.[8–10] Cramer's group synthesized hydroxylamines through the protonation of oxime using protonic acid while stabilizing the N−O bond over Ir complex.[11] A Lewis and Brønsted acid cooperation strategy was developed for hydrogenation of oximes, achieving high conversion and selectivity for hydroxylamines synthesis.[12] Besides H_2, $NaBH_3CN$ and BH_3 have been identified as efficient reagents that smoothly reduced oximes to alkylhydroxylamines.[13,14] The emergence of the concept of green chemistry has compelled individuals to seek more sustainable methodologies for addressing environmental pollution and climate change.[15–25]

Electrocatalytic hydrogenation (ECH) has emerged as a promising alternative, leveraging clean and pollution-free electricity as the driving force. This process utilizes protons and electrons to circumvent H_2 and other reductants.[26–35] Electrochemistry has been demonstrated great potential in the synthesis of high value-added chemicals,[36–46] such as ethylbenzene from styrene,[47] ethylene from acetylene,[48] succinic acid from maleic acid,[49] and furfuryl alcohol from furfuraldehyde.[50,51] Recent advances have demonstrated the ECH of oximes to amino acids under mild conditions,[52–54] which bring novel insights for hydroxylamines synthesis. However, the selective generation of hydroxylamines remains an unexplored area. The challenge lies in modulating electron transfer kinetics to stabilize the N−O moiety while avoiding over-reduction to amines—a process requiring precise interfacial control of adsorbed intermediates. Addressing this gap necessitates a fundamental re-examination of oxime activation mechanisms and ingenious catalyst design for catalytic sites–substrate interactions under electrochemical bias. To the best of our knowledge, no electrocatalytic system has been successfully applied to hydrogenation of oximes for

[*] S. Li[+], P. Liao[+], J. Li[+], P. Jiang[+], R. Xiang, Prof. G. Li
MOE Laboratory of Bioinorganic and Synthetic Chemistry, GBRCE for Functional Molecular Engineering, Lehn Institute of Functional Materials, School of Chemistry, Sun Yat-Sen University, Guangzhou 510006, China
E-mail: liguangqin@mail.sysu.edu.cn

P. Jiang[+]
BYD Auto Industry Company Limited, Shenzhen 518083, China

[+] These authors contributed equally to this work.

📖 Additional supporting information can be found online in the Supporting Information section
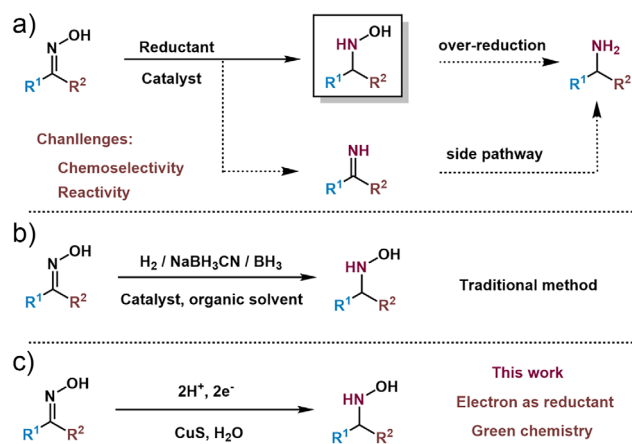
Scheme 1. a) Synthetic routes and challenges in catalytic reduction of oximes to hydroxylamine products; b) hydroxylamine synthesis by conventional method; c) hydroxylamine synthesis by electrochemical method in this work.

hydroxylamines synthesis, primarily due to the instability of the N—O bond under reductive conditions.

Herein, we report the first electrocatalytic method for the reduction of oximes to hydroxylamines. By designing a CuS-based catalyst with tailored adsorption sites and optimized dynamics of proton transfer, we achieve a high conversion and product selectivity for *N*-benzylhydroxylamine synthesis at −0.9 V versus reversible hydrogen electrode (RHE). The catalytic system could be operated in a stable cycle, which was also applicable for the synthesis of other hydroxylamines. This work advances hydroxylamine synthesis through a green-efficient electrosynthetic platform avoiding the use of reducing reagents, offering a blueprint for next-generation green and sustainable organic electrosynthetic strategies.

Results and Discussion

In particular, the fresh, highly crystalline, and purified CuS nanoparticles were fabricated via a controlled hydrothermal synthesis approach at 180 °C for 24 h, utilizing copper acetate and thioacetamide as precursors. According to the powder X-ray diffraction pattern (XRD) result (Figure 1a), CuS nanoparticles showed sharp peaks at about 29.3°, 31.8°, and 47.9°, which were corresponding to (102), (103), and (110) lattice planes of CuS,[55] respectively. As illustrated in Figure S1, scanning electron microscopy (SEM) revealed that the morphologies of the CuS nanoparticles exhibited an average particle size of 50 nm. Furthermore, high-resolution transmission electron microscopy (HRTEM, Figure 1b,c) revealed the presence of well-defined lattice spacing distances of 0.28 and 0.33 nm, corresponding to the (103) and (100) planes of CuS.[56] Aberration-corrected high-angle annular dark-field scanning transmission electron microscopy (HAADF-STEM) and energy dispersion X-ray spectroscopy (EDX) mappings (Figure 1d) further indicate that Cu and S elements are uniformly distributed in each nanoparticle, confirming the successful formation of CuS nanoparticles.

To assess the electrocatalytic performance, the as-synthesized CuS nanoparticles were uniformly deposited onto carbon cloth substrate via drop-casting, which was employed as a working electrode. The hydrogenation of oximes to hydroxylamines was investigated through chronoamperometric measurements at controlled potentials in a three-electrode system (H-type cell). Benzaldoxime is one of the simplest and most commonly used aromatic oximes in industry. Therefore, benzaldoxime was initially chosen as the model substance for hydroxylamines electrosynthesis (Figure 2a), as detailed in the experimental methods section. The electrolyte after electrosynthesis was analyzed by ^{1}H-nuclear magnetic resonance (^{1}H NMR). As displayed in Figure S2, a single peak observed at around 4.31 ppm was assigned to the proton on the α-carbon of *N*-benzylhydroxylamine, which was consistent with the peak position of commercial *N*-benzylhydroxylamine. Therefore, the successful electrocatalytic synthesis of *N*-benzylhydroxylamine was confirmed. Meanwhile, benzylamine was also detected and quantified by ^{1}H NMR analysis.

Encouragingly, the as synthesized *N*-benzylhydroxylamine on CuS, corresponding a selectivity of 80%, is far superior to that on carbon cloth matrix, Cu, Cu$_2$O, and CuO (Figures 2b and S3–S6). The performance of a series of metal foils (Fe, Co, Ni, Cu, Zn, Figures S7–S11) were also investigated. Among these metals foil catalysts, Cu demonstrated the highest selectivity (34%) for *N*-benzylhydroxylamine, and a 4357 μmol L^{-1} h^{-1} yield rate (Figure 2c). In contrast, no *N*-benzylhydroxylamine was detected with the Zn catalyst. For Co, Fe, and Ni, the selectivity for *N*-benzylhydroxylamine did not exceed 5%. The remarkable performance of Cu may be attributed to its unique electronic structure, which facilitates the stabilization of N—O intermediates. To our astonishment, the catalytic system could operate in continuous cycles for 260 h with negligible activity decay, indicating the superiority of this electrocatalytic system (Figures 2d and S12).

Due to the specific activity of CuS, further investigations were carried out to explore the influence factors on electrochemical reduction of oxime system, which was used to understand the catalytic process and mechanism of hydroxylamine formation over CuS. Linear scanning voltammetry (LSV) was initially conducted in an argon-saturated 0.05 M H$_2$SO$_4$ electrolyte (Figure S13). A notable increase in current density was observed following the addition of benzaldoxime to the system, indicating that benzaldoxime may react rapidly on the surface of CuS. As illustrated in Figure S14, at the open-circuit voltage, no hydrogenation products, such as hydroxylamine and amine, were detected. This observation suggests that electricity acts as the driving force behind the synthesis of hydroxylamine. By controlling the potential, the conversion of oxime increases with the increase of voltage (Figures S2 and S15–S20, from −0.5 to −1.3 V versus RHE), while the selectivity of *N*-benzylhydroxylamine formation increases slowly at first and then decreases sharply. The catalytic system reaches a peak value at −0.9 V versus RHE, indicating the necessity for an appropriate energy supply. Excessively high voltage may lead to the cleavage of the N—O bond. By controlling the voltage, a high selection of synthetic target products can be achieved. Furthermore,
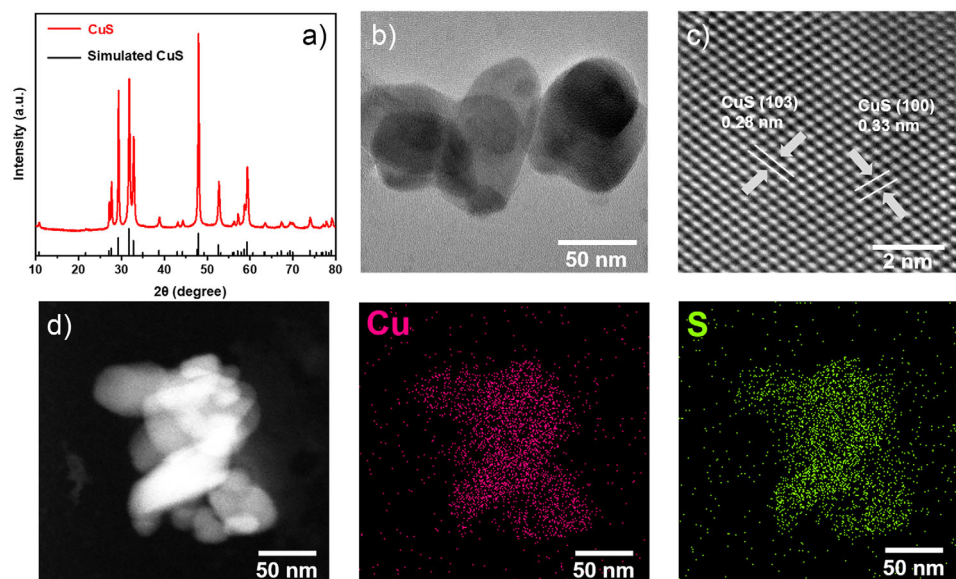
Angew. Chem. Int. Ed. **2025**, e202507853 (2 of 7)

© 2025 Wiley-VCH GmbH

Figure 1. Characterizations of CuS. a) Powder XRD pattern of as synthesized CuS; b,c) HRTEM and d) HAADF-STEM images of CuS with corresponding EDX mappings of Cu and S elements.
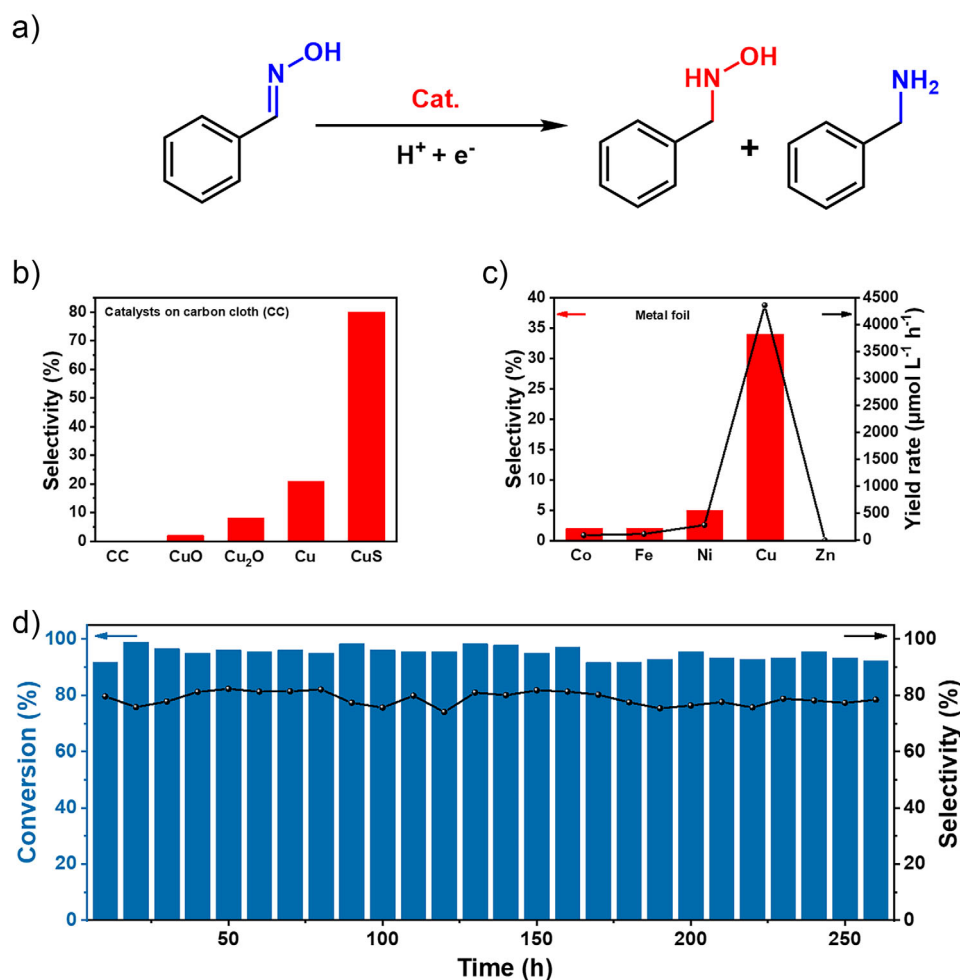

Figure 2. The performance of electrosynthesizing hydroxylamines. a) Schematic illustration of the transformation from benzaldoxmine to *N*-benzylhydroxylamine; b) the performance comparison of different copper based catalyst on carbon cloth in electrosynthesizing *N*-benzylhydroxylamine at −0.9 V versus RHE; c) the performance comparison of different metal foils in electrosynthesizing *N*-benzylhydroxylamine at −0.9 V versus RHE; d) the long-term stability test for *N*-benzylhydroxylamine production on CuS.
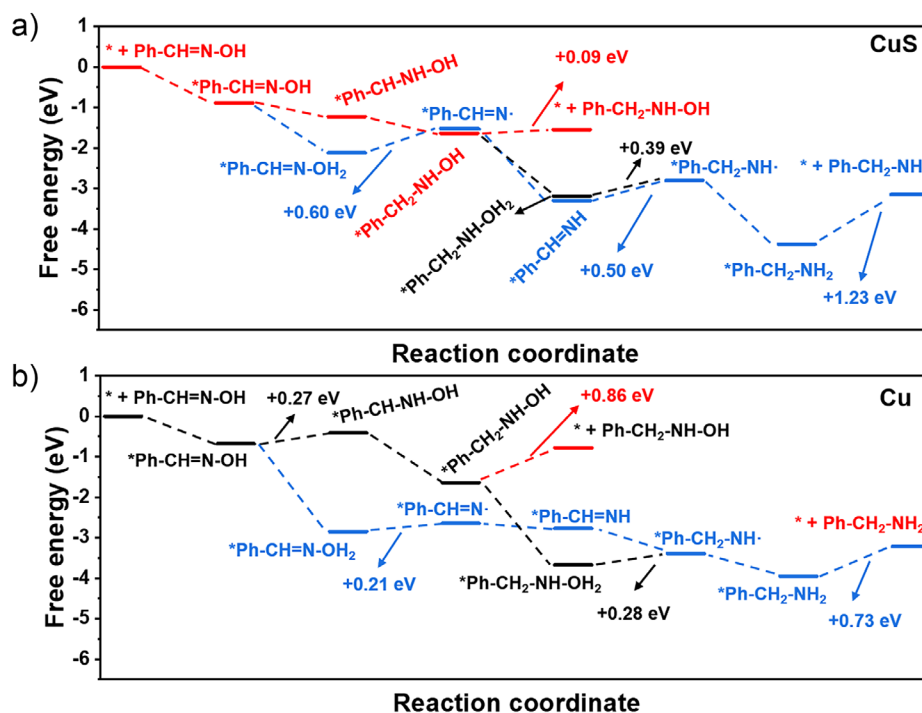
Figure 3. DFT calculations. The free-energy diagram for selective hydrogenation of benzaldoxime on the surface of a) CuS and b) Cu.

the impact of temperature (ranging from 4 to 50 °C, as shown in Figures S21–S23) on this reaction was investigated. The experimental results indicated that selectivity was significantly enhanced at lower temperatures, while the conversion remained relatively unaffected. This phenomenon could be attributed to the instability of the N—O bond under elevated temperatures. The high activation energy (voltage) and thermal excitation would promote N—O bond cleavage, thereby increasing the probability of amine by-product formation through alternative decomposition pathways. The input energy can be meticulously regulated through electrochemical processes, enabling the adjustment of reaction selectivity while simultaneously minimizing energy consumption.
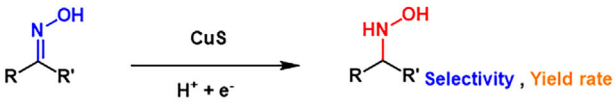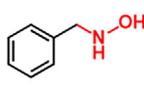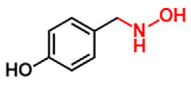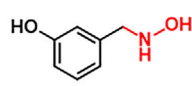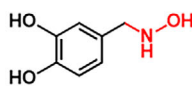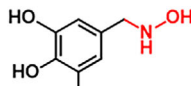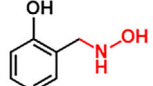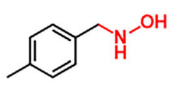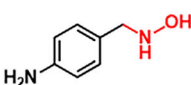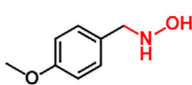
In addition, electrochemical evaluations conducted under varied pH conditions revealed a pronounced dependence of hydroxylamine formation efficiency on proton concentration. As demonstrated in Figures S24–S27, the reaction exhibited a maximum selectivity (80%) at pH = 1. While at pH = 0, the selectivity was decreased to 40%, indicating the existence of an optimal proton concentration window for this proton-coupled electron transfer process. The diminished yields observed under neutral (pH = 7) and alkaline (pH = 13) conditions, suggest kinetic limitations arising from insufficient proton availability for sequential protonation steps. Active hydrogen (*H) might play an important ro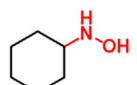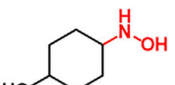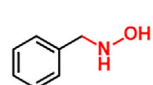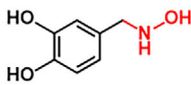le in the electrohydrogenation reaction. The importance of *H in hydroxylamine electrosynthesis was demonstrated by the introduction of hydroquinone as a free radical inhibitor to trap the *H species (Figures S28 and S29), which resulted in a significant decrease of N-benzylhydroxylamine yield. Kinetic analysis of the reaction revealed that the formation processes of both hydroxylamine and amine followed first-order reaction kinetics, with the rate of N-benzylhydroxylamine

formation being significantly higher than that of benzylamine (Figures S2, S30–S34). The electrochemical analysis reveals that the catalytic pathway favors hydroxylamines generation on the CuS surface in comparison to amine formation.

To understand the catalytic sites of CuS, controlled electrocatalytic evaluations employing S and a series of sulfides as reference catalysts revealed markedly inferior N-benzylhydroxylamine production rates (Figures S35–S40), indicating that the active sites are Cu species. By comparing the LSV curves (Figure S41), it was found that the current of CuS is smaller than Cu at the same potential, which may be due to the insertion of sulfur, inhibiting excessive hydrogenation.

To clarify the differences of electronic structure between Cu and CuS, X-ray photoelectron spectroscopy (XPS, Figure S42) was carried out. The C $1s$ at 284.8 eV was employed as a reference for binding energy calibration.[57] The Cu $2p_{3/2}$ region of CuS displays two distinct peaks at 932.5 and 933.5 eV (Figure S43a), corresponding to monovalent (Cu$^+$) and divalent (Cu^{2+}) states, respectively. This assignment was corroborated by the Cu Auger *LMM* spectral features (Figure S44). The S $2p$ spectrum (Figure S43b) exhibits distinct characteristic peaks at 161.7 eV (Cu—S) and 162.5 eV (S—S), confirming the successful sulfide formation.[58] In the face-centered cubic (*fcc*) structure of metallic Cu, each Cu atom is equidistantly coordinated with 12 neighboring Cu atoms, forming a highly symmetrical three-dimensional (3D) network. All Cu atoms equally share an electron cloud. In contrast,[59,60] in CuS, S acts as a central bridging atom that connects to multiple Cu ions through ionic-covalent mixed bonds to construct a 3D network.[61] This localized bonding restricts electron migration and may play a crucial role in the

Table 1: Molecular structures of the desired hydroxylamine products and corresponding selectivity and yield rate through electrosynthesis.

1, **80%** , 1210 µmol L^{-1} h^{-1}

2, **82%** , 1210 µmol L^{-1} h^{-1}

3, **77%** , 1178 µmol L^{-1} h^{-1}

4, **88%** , 1220 µmol L^{-1} h^{-1}

5, **80%** , 1145 µmol L^{-1} h^{-1}

6, **71%** , 1036 µmol L^{-1} h^{-1}

7, **78%** , 1041 µmol L^{-1} h^{-1}

8, **63%** , 885 µmol L^{-1} h^{-1}

9, **66%** , 1017 µmol L^{-1} h^{-1}

10, **99%** , 1112 µmol L^{-1} h^{-1}

11, **90%** , 1130 µmol L^{-1} h^{-1}

1a, **40%** , 165 µmol L^{-1} h^{-1} [NO]

4a, **45%** , 161 µmol L^{-1} h^{-1} [NO]

electrohydrogenation synthesis of hydroxylamine due to its unique structural characteristics.

Based on the above experimental results, density functional theory (DFT) calculations were further performed to understand the mechanism in the hydrogenation process on Cu (111) and CuS (110) surfaces according to the XRD patterns and HRTEM images, and the models were constructed. The hydrogenation energy of different reaction pathways were calculated to understand the selective hydrogenation of benzaldoxime (Figure 3). Specifically, the hydrogenation of oximes typically proceeds through intermediates such as imines or transient hydroxylamines, ultimately yielding primary amines. However, for CuS, the rate-determining step (RDS) energy of the formation of *N*-benzylhydroxylamine is only 0.09 eV. Meanwhile, the energy for further hydrogenation to *Ph-CH$_2$-NH• from *Ph-CH$_2$-NH-OH$_2$ is 0.39 eV, and the RDS energy on the way to Ph-CH$_2$-NH$_2$ is 1.23 eV (the desorption of *Ph-CH$_2$-NH$_2$). Hence, *N*-benzylhydroxylamine is the favorable target product in the hydrogenation steps over CuS. In stark contrast, the reaction RDS energy for the hydroxylamine formation

pathway involving Cu is 0.86 eV, while the energy for amine formation is slightly lower at 0.73 eV when proceeding through the imines pathway. The result is coincided with the experiment result that amine product is the main product over Cu surface. It is noted that the formation of benzylamine can go through the *N*-benzylhydroxylamine over CuS and Cu surface, but it requires to cross a higher energy barrier compared with the imine pathway. The control experiments further support this mechanistic interpretation. Utilizing *N*-benzylhydroxylamine as the substrate, we observed a low yield of 10% for Cu and 12% for CuS to benzylamine at −0.9 V versus RHE under 4 °C over a duration of 10 h. In contrast, at 25 °C, the yields were improved to 29% and 18%, respectively, as quantified by ^{1}H NMR analysis (Figures S45–S49).

To elucidate the catalyst–reactant electronic interactions, differential charge density and Bader charge analysis were conducted for benzaldoxime adsorbed on both CuS and metallic Cu surfaces. As shown in Figures S50 and S51, there was a clear charge transfer between Cu and N in differential charge density result, indicating that adsorption

Angew. Chem. Int. Ed. **2025**, e202507853 (5 of 7)

© 2025 Wiley-VCH GmbH

occurred between Cu and N of benzaldoxime and that electrons flowed from Cu to N. The adsorption energy analysis of *Ph-CH$_2$-NH-OH on CuS is significantly close to 0 eV when compared to that on Cu (Figure S52), making it more difficult to be activated for reductive cleavage.[62,63] The *Ph-CH$_2$-NH-OH is prone to desorption on CuS rather than further hydrogenation to form amines, thus resulting in a high selectivity.

To evaluate the reactant substrate generality of this electrocatalytic methodology, a series of aldoxime and ketoxime derivatives were systematically investigated under the optimized reaction conditions. As detailed in Table 1 and Table S1, 11 kinds of hydroxylamines bearing different substituents, such as –OH, –CH$_3$, –NH$_2$, were successfully synthesized, with product identities unambiguously confirmed by ^{1}H NMR spectroscopy and liquid chromatography–mass spectrometry (Figures S53–S71). We further scaled up the experiment at the laboratory level (Figure S72) to investigate the potential for industrial application of this method. Notably, 1.04 g of *N*-benzylhydroxylamine was produced within 10 h in a 0.5 L electrolytic cell. Notably, this platform enabled the tandem electrochemical synthesis of organic hydroxylamine through in situ coupling of nitric oxide (NO) (Figures S73 and S74), establishing a novel pathway for valorizing waste nitrogen oxides into value-added organic hydroxylamines. Remarkably, despite the existence of multiple competing electron transfer pathways in the NO to hydroxylamine conversion process, our approach demonstrated a notable product selectivity of ≥ 40%. Therefore, this robust synthetic methodology held a great potential for the production of hydroxylamine derived from nitrogen oxides and ketones through operationally straightforward and safe electrochemical processes. All these results indicated that the developed strategy and catalysts had broad application prospects. Although the Faraday efficiency of the current electrocatalytic system remains relatively low, it is anticipated that future in-depth research will lead to significant improvements.

Conclusion

In summary, we demonstrate a robust electrocatalytic strategy that directly converts oximes to hydroxylamines with exceptional selectivity and efficiency under mild conditions. By rational design of a CuS-based catalyst with tailored adsorption sites and precise modulation of proton activity, we achieve a high selectivity and yield for *N*-benzylhydroxylamine at a low applied potential, coupled with remarkable stability over 260 h. Mechanistic studies unveil that CuS can optimize the adsorption energy of the reaction intermediates, making the N─O bond more difficult to cleave during the electrocatalytic hydrogenation, thus leading to a highly selective formation of hydroxylamines. The versatility of this approach is underscored by its successful extension to 11 structurally diverse hydroxylamines and the groundbreaking synthesis of organic hydroxylamines directly from NO, a previously unexplored route. Therefore, this work provides fundamental insights into controlling redox cascades through coordinated chemistry, offering a blueprint

for designing selective electrocatalytic systems. This advance not only addresses a critical gap in amine and hydroxylamine chemistry, but also opens avenues for exploring radical-mediated functional materials in organic electrosynthesis.

Conflict of Interests

The authors declare no conflict of interest.

Data Availability Statement

The data that support the findings of this study are available from the corresponding author upon reasonable request.

[1] P. Gross, *Crit. Rev. Toxicol.* **1985**, *14*, 87–99.

[2] M. Zhu, X. Zhang, C. Zheng, S.-L. You, *ACS Catal.* **2020**, *10*, 12618–12626.

[3] M. P. Paudyal, A. M. Adebesin, S. R. Burt, D. H. Ess, Z. Ma, L. Kürti, J. R. Falck, *Science* **2016**, *353*, 1144–1147.

[4] T. Song, Y. Luo, K. Wang, B. Wang, Q. Yuan, W. Zhang, *ACS Catal.* **2023**, *13*, 4409–4420.

[5] C. Ciotonea, N. Hammi, J. Dhainaut, M. Marinova, A. Ungureanu, A. El Kadib, C. Michon, S. Royer, *ChemCatChem.* **2020**, *12*, 4652–4663.

[6] J. Mas-Rosello, N. Cramer, *Chemistry* **2022**, *28*, e202103683.

[7] J. Chen, H. Wei, I. D. Gridnev, W. Zhang, *Angew. Chem. Int. Ed.* **2025**, e202425589.

[8] B. Li, J. Chen, D. Liu, I. D. Gridnev, W. Zhang, *Nat. Chem.* **2022**, *14*, 920–927.

[9] P. Li, E. Zheng, G. Li, Y. Luo, X. Huo, S. Ma, W. Zhang, *Science* **2024**, *385*, 972–979.

[10] Z. Wu, J. Meng, H. Liu, Y. Li, X. Zhang, W. Zhang, *Nat. Chem.* **2023**, *15*, 988–997.

[11] J. Mas-Roselló, T. Smejkal, N. Cramer, *Science* **2020**, *368*, 1098–1102.

[12] F. Wang, Y. Chen, P. Yu, G.-Q. Chen, X. Zhang, *J. Am. Chem. Soc.* **2022**, *144*, 17763–17768.

[13] M. Morimoto, W. Cao, R. G. Bergman, K. N. Raymond, F. D. Toste, *J. Am. Chem. Soc.* **2021**, *143*, 2108–2114.

[14] R. F. Borch, M. D. Bernstein, H. D. Durst, *J. Am. Chem. Soc.* **1971**, *93*, 2897–2904.

[15] Y. Fan, Y. Jiang, H. Lin, J. Li, Y. Xie, A. Chen, S. Li, D. Han, L. Niu, Z. Tang, *Nat. Commun.* **2024**, *15*, 4679.

[16] Y. Fan, W. Zhou, X. Qiu, H. Li, Y. Jiang, Z. Sun, D. Han, L. Niu, Z. Tang, *Nat. Sustain.* **2021**, *4*, 509–515.

[17] J. Li, T. Xiang, X. Liu, M. N. Ghazzal, Z.-Q. Liu, *Angew. Chem. Int. Ed.* **2024**, *63*, e202407287.

[18] S. Kaushik, D. Wu, Z. Zhang, X. Xiao, C. Zhen, W. Wang, N.-Y. Huang, M. Gu, Q. Xu, *Adv. Mater.* **2024**, *36*, 2401163.

[19] C. Yang, X. Li, Y. Liang, *Inorg. Chem. Front.* **2023**, *10*, 5517–5554.

[20] Y. Zhen, C. Yang, H. Shen, W. Xue, C. Gu, J. Feng, Y. Zhang, F. Fu, Y. Liang, *Phys. Chem. Chem. Phys.* **2020**, *22*, 26278–26288.

[21] D. Xia, Q. Chen, Y. Jiao, Q. Lian, M. Sun, C. He, J. Shang, T. Wang, *Water Res.* **2022**, *217*, 118423.

[22] J. Jiao, W. Qiu, J. Tang, L. Chen, L. Jing, *Nano Res.* **2016**, *9*, 1256–1266.

[23] H. Minamihara, K. Kusada, D. Wu, T. Yamamoto, T. Toriyama, S. Matsumura, L. S. R. Kumara, K. Ohara, O. Sakata, S. Kawaguchi, Y. Kubota, H. Kitagawa, *J. Am. Chem. Soc.* **2022**, *144*, 11525–11529.

[24] D. Wu, K. Kusada, S. Yoshioka, T. Yamamoto, T. Toriyama, S. Matsumura, Y. Chen, O. Seo, J. Kim, C. Song, S. Hiroi, O. Sakata, T. Ina, S. Kawaguchi, Y. Kubota, H. Kobayashi, H. Kitagawa, *Nat. Commun.* **2021**, *12*, 1145.

[25] J. Jiao, Y. Ma, X. Han, A. Ergu, C. Zhang, P. Chen, W. Liu, Q. Luo, Z. Shi, H. Xu, C. Chen, Y. Li, T. Lu, *Nat. Commun.* **2025**, *16*, 857.

[26] Y. Zeng, M. Zhao, H. Zeng, Q. Jiang, F. Ming, K. Xi, Z. Wang, H. Liang, *eScience.* **2023**, *3*, 100156.

[27] H. Li, Y. Li, J. Chen, L. Lu, P. Wang, J. Hu, R. Ma, Y. Gao, H. Yi, W. Li, A. Lei, *Angew. Chem. Int. Ed.* **2024**, *63*, e202407392.

[28] K. Dong, Y. Yao, H. Li, H. Li, S. Sun, X. He, Y. Wang, Y. Luo, D. Zheng, Q. Liu, Q. Li, D. Ma, X. Sun, B. Tang, *Nat. Synth.* **2024**, *3*, 763–773.

[29] M. Dan, R. Zhong, S. Hu, H. Wu, Y. Zhou, Z.-Q. Liu, *Chem Catal* **2022**, *2*, 1919–1960.

[30] S. A. Akhade, N. Singh, O. Y. Gutiérrez, J. Lopez-Ruiz, H. Wang, J. D. Holladay, Y. Liu, A. Karkamkar, R. S. Weber, A. B. Padmaperuma, M.-S. Lee, G. A. Whyatt, M. Elliott, J. E. Holladay, J. L. Male, J. A. Lercher, R. Rousseau, V.-A. Glezakou, *Chem. Rev.* **2020**, *120*, 11370–11419.

[31] X. Kong, J. Ni, Z. Song, Z. Yang, J. Zheng, Z. Xu, L. Qin, H. Li, Z. Geng, J. Zeng, *Nat. Sustain.* **2024**, *7*, 652–660.

[32] J. Jiao, Q. Yuan, M. Tan, X. Han, M. Gao, C. Zhang, X. Yang, Z. Shi, Y. Ma, H. Xiao, J. Zhang, T. Lu, *Nat. Commun.* **2023**, *14*, 6164.

[33] N. Sun, S. Ru, C. Zhang, W. Liu, Q. Luo, J. Jiao, T. Lu, *Fund Res-China* **2022**, https://doi.org/10.1016/j.fmre.2022.07.014.

[34] M. Zheng, J. Zhang, P. Wang, H. Jin, Y. Zheng, S.-Z. Qiao, *Adv. Mater.* **2024**, *36*, 2307913.

[35] Y. Zeng, M. Zhao, H. Zeng, Q. Jiang, F. Ming, K. Xi, Z. Wang, H. Liang, *eScience* **2023**, *3*, 100156.

[36] Y. Fu, X. Yang, Y. Yu, K. Zhou, X. Ye, A. Zhang, X. Hou, B. Chen, F. Fan, Y. Li, Y. Fu, *Nano Res.* **2025**, *18*, 94907038.

[37] W. He, X. Li, X. Dai, L. Shao, Y. Fu, D. Xu, W. Qi, *Angew. Chem. Int. Ed.* **2024**, *63*, e202411539.

[38] Y. Tian, H. Wu, A. Hanif, Y. Niu, Y. Yin, Y. Gu, Z. Chen, Q. Gu, Y. H. Ng, J. Shang, L. Li, M. Liu, *Chin. Chem. Lett.* **2023**, *34*, 108056.

[39] X. Fan, C. Liu, X. He, Z. Li, L. Yue, W. Zhao, J. Li, Y. Wang, T. Li, Y. Luo, D. Zheng, S. Sun, Q. Liu, L. Li, W. Chu, F. Gong, B. Tang, Y. Yao, X. Sun, *Adv. Mater.* **2024**, *36*, 2401221.

[40] H. Zhang, H. Wang, X. Cao, M. Chen, Y. Liu, Y. Zhou, M. Huang, L. Xia, Y. Wang, T. Li, D. Zheng, Y. Luo, S. Sun, X. Zhao, X. Sun, *Adv. Mater.* **2024**, *36*, 2312746.

[41] T. Xie, X. He, L. He, K. Dong, Y. Yao, Z. Cai, X. Liu, X. Fan, T. Li, D. Zheng, S. Sun, L. Li, W. Chu, A. Farouk, M. S. Hamdy, C. Xu, Q. Kong, X. Sun, *Chin. Chem. Lett.* **2024**, *35*, 110005.

[42] J. Jiao, R. Lin, S. Liu, W.-C. Cheong, C. Zhang, Z. Chen, Y. Pan, J. Tang, K. Wu, S.-F. Hung, H. M. Chen, L. Zheng, Q. Lu, X. Yang, B. Xu, H. Xiao, J. Li, D. Wang, Q. Peng, C. Chen, Y. Li, *Nat. Chem.* **2019**, *11*, 222–228.

[43] J. Jiao, W. Yang, Y. Pan, C. Zhang, S. Liu, C. Chen, D. Wang, *Small* **2020**, *16*, 2002124.

[44] M. Qi, Y. Ma, C. Zhang, B. Li, X. Yang, Z. Shi, S. Liu, C. An, J. Jiao, T. Lu, *Sci. China Chem.* **2025**, *68*, 1620–1626.

[45] X. Peng, L. Wen, Z. Ning, Z. Zhang, C. Sun, Y. Tang, P. Feng, *Org. Chem. Front.* **2022**, *9*, 3800–3806.

[46] Z. Zhang, L. Wen, S. Xu, Y. Tang, X. Cao, P. Feng, *Green Chem.* **2023**, *25*, 2287–2292.

[47] C. Han, J. Zenner, J. Johny, N. Kaeffer, A. Bordet, W. Leitner, *Nat. Catal.* **2022**, *5*, 1110–1119.

[48] W. Xue, X. Liu, C. Liu, X. Zhang, J. Li, Z. Yang, P. Cui, H.-J. Peng, Q. Jiang, H. Li, P. Xu, T. Zheng, C. Xia, J. Zeng, *Nat. Commun.* **2023**, *14*, 2137.

[49] G. Han, G. Li, Y. Sun, *Nat. Catal.* **2023**, *6*, 224–233.

[50] Z.-C. Yao, J. Chai, T. Tang, L. Ding, Z. Jiang, J. Fu, X. Chang, B. Xu, L. Zhang, J.-S. Hu, L.-J. Wan, *Proc. Natl. Acad. Sci. USA* **2025**, *122*, e2423542122.

[51] N.-Y. Huang, B. Chu, D. Chen, B. Shao, Y.-T. Zheng, L. Li, X. Xiao, Q. Xu, *J. Am. Chem. Soc.* **2025**, *147*, 8832–8840.

[52] T. Fukushima, M. Yamauchi, *J. Appl. Electrochem.* **2021**, *51*, 99–106.

[53] P. Liao, B. Zeng, S. Li, Y. Zhang, R. Xiang, J. Kang, Q. Liu, G. Li, *Angew. Chem. Int. Ed.* **2025**, *64*, e202417130.

[54] T. Fukushima, M. Yamauchi, *Chem Commun (Camb)* **2019**, *55*, 14721–14724.

[55] W. Zhao, X. Wang, X. Ma, L. Yue, Y. Ren, T. Li, J. Xia, L. Zhang, Q. Liu, Y. Luo, N. Li, B. Tang, Y. Liu, S. Gao, A. M. Asiri, X. Sun, *J. Mater. Chem. A* **2021**, *9*, 27615–27628.

[56] Y. Wang, D. Chao, Z. Wang, J. Ni, L. Li, *ACS Nano* **2021**, *15*, 5420–5427.

[57] T. Ouyang, X. T. Wang, X. Q. Mai, A. N. Chen, Z. Y. Tang, Z. Q. Liu, *Angew. Chem. Int. Ed.* **2020**, *59*, 11948–11957.

[58] J. Zhang, L. Duan, W. Zhang, B. Ma, J. Zhang, J. Li, A. Wang, P. Guo, D. Zhao, Y. Ma, *Angew. Chem. Int. Ed.* **2025**, *64*, e202423861.

[59] K. Jiang, Z. Chen, X. Meng, *ChemElectroChem* **2019**, *6*, 2825–2840.

[60] F. Jamal, A. Rafique, S. Moeen, J. Haider, W. Nabgan, A. Haider, M. Imran, G. Nazir, M. Alhassan, M. Ikram, Q. Khan, G. Ali, M. Khan, W. Ahmad, M. Maqbool, *ACS Appl. Nano Mater* **2023**, *6*, 7077–7106.

[61] L. Isac, C. Cazan, L. Andronic, A. Enesca, *Catalysts* **2022**, *12*, 1135.

[62] B. Peng, H. She, Z. Wei, Z. Sun, Z. Deng, Z. Sun, W. Chen, *Nat. Commun.* **2025**, *16*, 2217.

[63] Y. Guo, Y. Huang, B. Zeng, B. Han, M. Akri, M. Shi, Y. Zhao, Q. Li, Y. Su, L. Li, Q. Jiang, Y.-T. Cui, L. Li, R. Li, B. Qiao, T. Zhang, *Nat. Commun.* **2022**, *13*, 2648.

Research Article

S. Li, P. Liao, J. Li, P. Jiang, R. Xiang,
G. Li* ——————— **e202507853**

Green Electrosynthesis of Hydroxylamines
via CuS Suppressing N—O Bond Cleavage

The electrocatalytic method for synthetic organic hydroxylamines was firstly reported from the reduction of oximes on a CuS catalyst. Mechanistic investigations revealed that CuS owns well absorption energy for N—O bond which is difficult for reductive cleavage, thus it could suppress over-hydrogenation. This work provides a blueprint for next-generation green and sustainable organic electrosynthetic strategies.